Available online at www.sciencedirect.com
ScienceDirect
Phytochemistry 68 (2007) 2330–2340
PHYTOCHEMISTRY
www.elsevier.com/locate/phytochem

NMR-based fluxomics: Quantitative 2D NMR methods for isotopomers analysis

Stéphane Massou [a,b], Cécile Nicolas [a], Fabien Letisse [a,b], Jean-Charles Portais [a,b,*]

[a] Laboratoire Biotechnologie – Bioprocédés, UMR INSA/CNRS 5504 INRA 792, LBB/INSA, 135 Avenue de Rangueil, 31077 Toulouse Cedex 4, France
[b] Université Paul Sabatier, 118 Route de Narbonne, 31062 Toulouse Cedex, France

Received 12 January 2007; received in revised form 3 March 2007
Available online 26 April 2007

Abstract

We have investigated the reliability of 2D-COSY and 2D-TOCSY experiments to provide accurate measurements of ^{13}C-enrichments in complex mixtures of ^{13}C-labelled metabolites. This was done from both theoretical considerations and experimental investigations. The results showed that 2D-TOCSY but not 2D-COSY could provide accurate measurements of ^{13}C-enrichments, provided efficient zero-quantum filters were applied during the mixing period. This approach extends the range of NMR methods applicable in ^{13}C-labelling experiments and is suitable to investigating the dynamic behaviour of metabolic systems.

Keywords: ^{13}C-labelling experiments; Quantitative 2D NMR; Specific ^{13}C-enrichments; 2D-COSY; 2D ZQF-TOCSY

1. Introduction

Over the past decades, NMR has been increasingly used to investigate carbon metabolism (Kelleher, 2001; Ratcliffe and Shachar-Hill, 2005, 2006; Shulman and Rothman, 2001). One of the most important applications lies in the analysis of metabolic fluxes from ^{13}C-labelling experiments (CLEs), where the distribution of carbon fluxes in complex metabolic networks can be estimated from the labelling pattern of metabolites (Wiechert, 2001). The size of the network that can be investigated in a CLE, as well as the accuracy on flux measurements, depend on the number and nature of the labelling data that are made available. NMR can provide two different types of data valuable for flux analysis: specific enrichments, i.e. the percentage of ^{13}C label incorporated in an individual carbon position of a metabolite, and isotopomers, i.e. the various isotopic isomers that can be generated for the same metabolite (Fig. 1). Specific enrichments are valuable for tracking the fate of individual carbon atoms in CLEs carried out with specifically-labelled substrate – e.g. [1-^{13}C]-glucose (Portais et al., 1993). Isotopomers provide detailed information regarding the breakdown or formation of carbon linkages in the metabolic network in CLEs carried out with mixtures of unlabelled and uniformly-labelled – like [U-^{13}C]glucose – substrates are considered. The two types of NMR data can be used independently for the purpose of flux analysis, but because they give complementary information regarding the structure and operation of metabolic networks, combinations of the two approaches can offer the optimal conditions for in-depth investigation of complex metabolic networks (Wittmann and Heinzle, 2001).

The measurement of isotopomers and specific enrichments relies on different NMR experiments (Szyperski, 1998). The isotopomer distribution can be extracted from the analysis of ^{13}C–^{13}C couplings in 1D ^{13}C or 2D ^{1}H–^{13}C NMR experiments (Szyperski, 1995; Carvalho et al., 1998; Burgess et al., 2001). 2D experiments are usually preferred over 1D experiments when complex mixtures of ^{13}C-labelled metabolites – such as cell extracts or biomass

* Corresponding author. Address: Laboratoire Biotechnologie – Bioprocédés, UMR INSA/CNRS 5504 INRA 792, LBB/INSA, 135 Avenue de Rangueil, 31077 Toulouse Cedex 4, France. Tel./fax: +33 561 55 96 89.
E-mail address: jean-charles.portais@insa-toulouse.fr (J.-C. Portais).

0031-9422/$ - see front matter © 2007 Elsevier Ltd. All rights reserved.
doi:10.1016/j.phytochem.2007.03.011

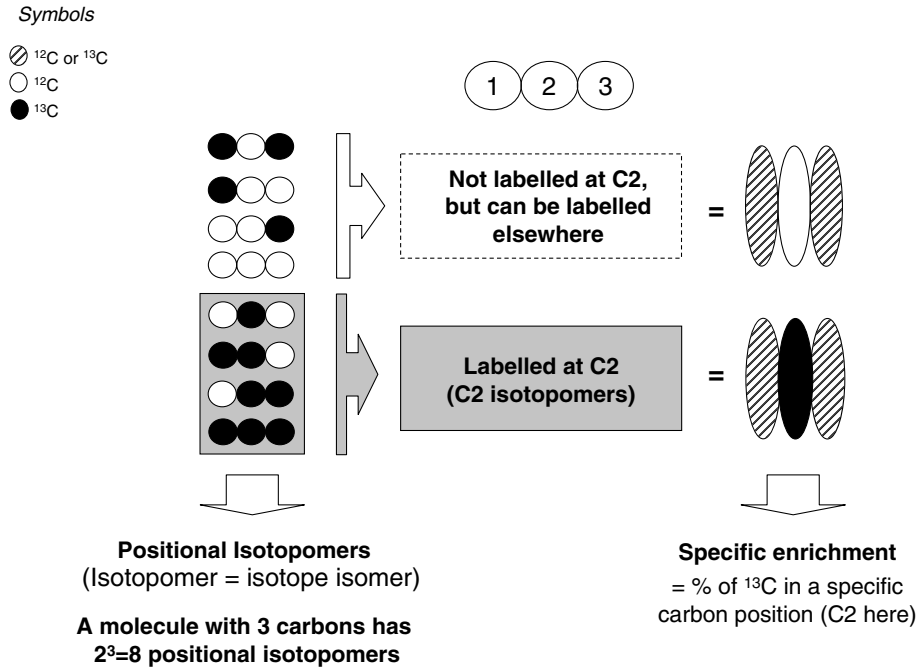

Fig. 1. Positional isotopomers and specific enrichment for a three-carbon fragment. In ^{13}C-labelling experiments, *positional isotopomers* (derived from isotopic isomers) usually refer the various isomers of a same molecule that differ in their carbon isotope composition (number of ^{13}C atoms) and positioning. Each carbon in a metabolite can be possibly labelled (^{13}C) or unlabelled (^{12}C), and a metabolite with n carbons has therefore 2^n positional isotopomers. This is illustrated here for a three-carbon fragment that has 8 positional isotopomers (left). *Specific enrichment* is the percentage of ^{13}C-atom in a specific carbon position of the metabolite. As illustrated for the C2 position, the 8 positional isotopomers of a three-carbon fragment can be grouped into 2 classes depending on the labelling state of C2: i.e. C2-labelled and C2-unlabelled isotopomers (right). The specific enrichment of C2 therefore corresponds also to the total fraction of C2-labelled isotopomers.

hydrolysates – are considered, and therefore, they are well suited for the investigation of large networks. The different types of 2D-^{13}C,^{1}H NMR experiments, e.g. HSQC, HMQC, etc. – that can be applied have been discussed in details in Szyperski (1998). The ^{13}C–^{13}C couplings useful for isotopomer analysis appear in the ^{13}C dimension of the spectrum. Because the signal originates from ^{13}C atoms only, the isotopomer distribution can be measured relative to the amount of label in the carbon position, but not as a percentage of the metabolite pool (Fig. 2). Such relative approach can be applied directly to situations where all the carbons have the same enrichment, i.e. in steady-state experiments carried out with uniformly-labelled (Szyperski, 1998), where the actual isotopomer distribution can be extracted by application of appropriate statistical treatment (Szyperski, 1995, 1998). It has been applied fruitfully to the analysis of steady-state metabolic fluxes in microbes (Szyperski, 1995), animals (Burgess et al., 2001; Carvalho et al., 1998) and plants (Sriram et al., 2004). But to examine combinations of labelled substrates or dynamic conditions, i.e. situations where the label does not incorporate equally in all carbon positions, the ^{13}C-enrichment of each carbon position of interest must be known to measure the actual isotopomer distribution as % of the total metabolite pool (Fig. 2). Specific enrichments can be measured from either 1D ^{1}H– or 2D ^{1}H–^{1}H NMR experiments. One-dimensional ^{1}H experiments have been widely applied in the CLEs (de Graaf et al., 2000; de Graaf, 2000). The application of 2D experiments has been quite limited so far and specific enrichments are usually measured from 1D NMR analyses carried out on purified metabolites (Alonso et al., 2005; Eisenreich et al., 2006; Rontein et al., 2002). But the process of metabolite purification can be tedious and is likely to be a limiting factor for extending further the size of metabolic networks that can be investigated. Therefore, there is a need for 2D-^{1}H,^{1}H NMR methods that provide accurate measurement of specific enrichments.

Two types of 2D ^{1}H–^{1}H NMR experiments are potentially attractive for the measurement of specific enrichments in complex mixtures of ^{13}C-labelled metabolites: COSY and TOCSY. These experiments are widely applied for the purpose of signal assignment, but there have been few attempts to apply them to measure specific ^{13}C-enrichments (Carvalho et al., 1998; Schmidt et al., 1999). In this work, we have investigated the reliability of 2D-COSY and 2D-TOCSY experiments to provide accurate measurements of ^{13}C-enrichments in complex mixtures of ^{13}C-labelled metabolites. This was done from both theoretical and experimental considerations. The results showed that 2D-TOCSY but not 2D-COSY could provide accurate measurements of ^{13}C-enrichments, provided efficient zero-quantum filters (Thrippleton and Keeler, 2003) were applied during the mixing period.

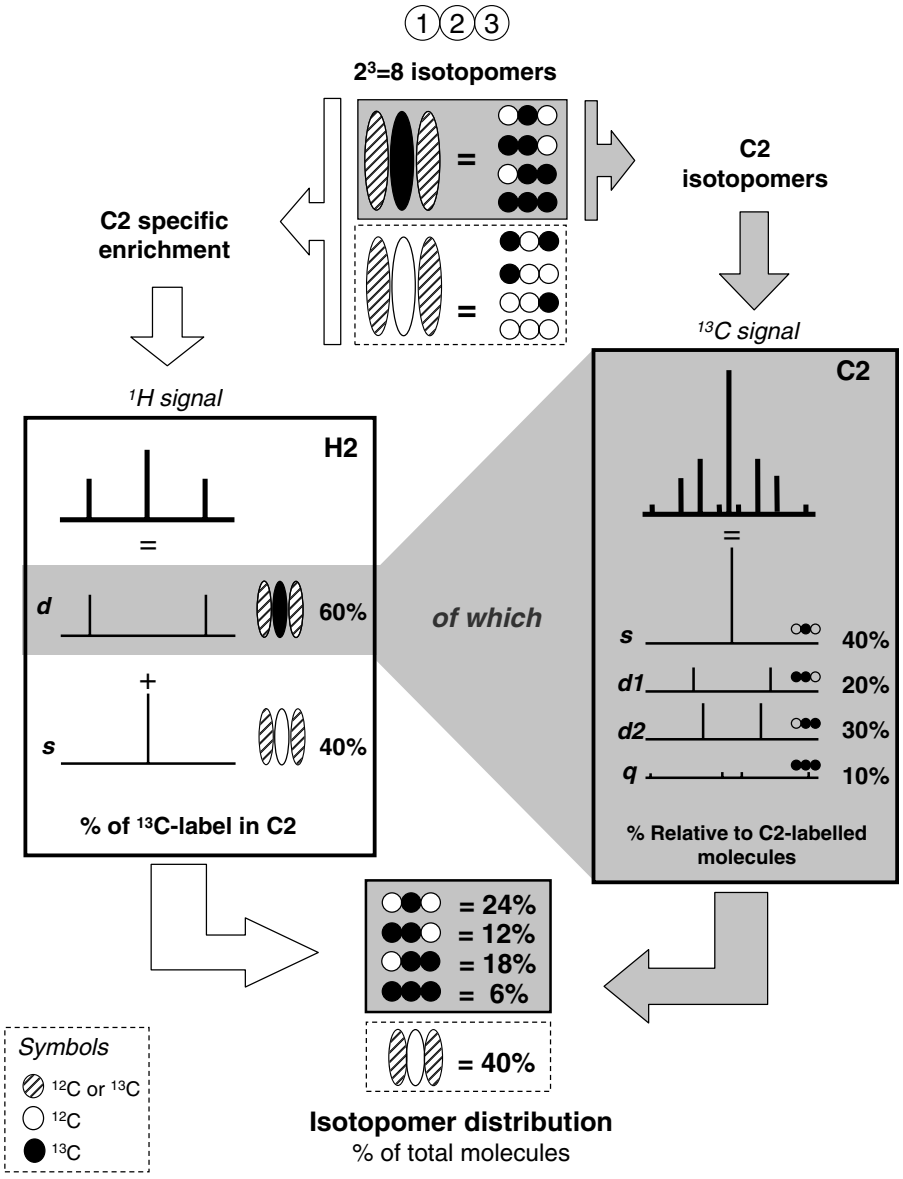

Fig. 2. Measurement of positional isotopomer distribution from a combination of ^{1}H and ^{13}C NMR experiments. The specific enrichment of the carbon C2 of a three-carbon fragment corresponds to the total fraction of all (positional) isotopomers labelled at C2 (top of the figure). When the C2 is protonated, its specific enrichment can be measured from the ^{1}H NMR analysis of the H2 protons. The H2 protons bound to a ^{12}C-atom give a singlet (s) meanwhile the H2 protons bound to a ^{13}C-atom give a doublet (d) due to scalar coupling. Because the signal intensity is proportional to the number of nuclei, the specific enrichment can be measured from the intensity of the doublet relative to the total intensity of the resonance. The distribution of C2-labelled isotopomers can be extracted from the ^{13}C NMR signal of the C2 carbon (right). Due to ^{13}C–^{13}C scalar couplings, the signal of the C2 carbon is influenced by the labelling state of the adjacent carbons. It is a singlet, a doublet, and a quadruplet if none, one or two of the adjacent carbons are labelled, respectively. The actual signal is the sum of the contributions from each individual isotopomer, and the abundance of the individual isotopomers can be determined from the integration of the various coupling structures. This abundance is expressed relative to the population of C2-labelled molecules. Because the specific enrichment of C2 represents the total fraction of all C2-labelled isotopomers, the abundance of each individual isotopomer can be expressed relative to the total amount of molecule by multiplying its relative abundance by the value of the specific enrichment (bottom). Therefore, the actual isotopomer distribution can be determined by combining ^{1}H and ^{13}C NMR. In practice, this can be achieved by using appropriate 1D or 2D NMR experiments, i.e. 1D ^{1}H or 2D-^{1}H,^{1}H experiments for measuring specific enrichments and 1D ^{13}C or 2D-^{13}C,^{1}H for measuring isotopomers.

2. Results and discussion

2.1. Interest of 2D homonuclear experiments

In a ^{1}H NMR spectrum, the signals from protons bound to a ^{12}C appear as center lines meanwhile the signal from protons attached to a ^{13}C nucleus appear as satellite lines due to the effects of heteronuclear scalar couplings (J_{CH}) (Fig. 3a). The relative ^{13}C content in the considered carbon position can be measured from the intensity of the satellite lines compared to the total intensity of the resonance. This method, although limited to protonated carbons, benefits from the NMR sensitivity of the ^{1}H nucleus much higher than that of the ^{13}C nucleus. The highest sensitivity can be

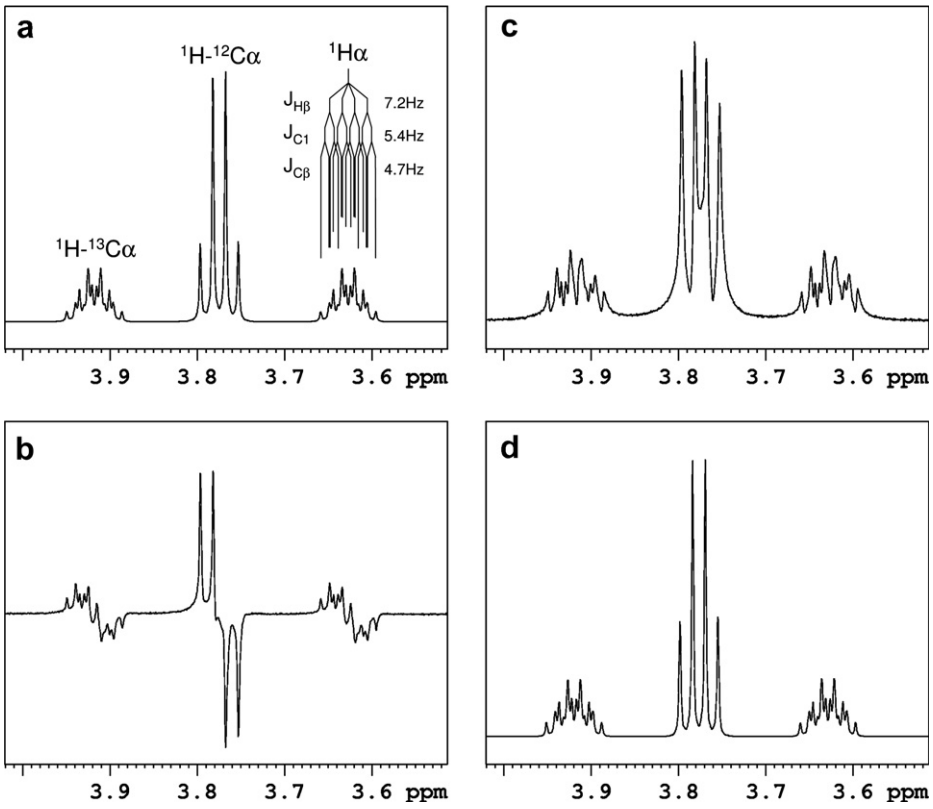

Fig. 3. Comparaison of Hα alanine signals in 1D ^{1}H, 2D DQF-COSY and 2D ZQF-TOCSY spectra recorded on a mixture of 50% unlabelled +50% [U-^{13}C]-alanine. Only the signals from the ^{1}Hα protons are displayed in the figure. (a) Peak from the 1D ^{1}H NMR spectrum, where the protons bound to a ^{13}C nucleus appear as satellite lines and the protons bound to a ^{12}C nucleus as a central quadruplet. The multiplicity of the satellite lines is detailed. The values of the heteronuclear coupling constants were determined from 1D selective ^{13}C-decoupling ^{1}H experiments. (b) Pseudo 1D spectrum obtained from the 2D COSY-DQF spectrum before magnitude correction. (c) Pseudo 1D spectrum obtained from the 2D COSY-DQF spectrum after magnitude correction. (d) Pseudo 1D spectrum obtained from the 2D ZQF-TOCSY spectrum. The 1D spectrum and the pseudo-spectra are displayed with the same chemical shift scale.

reached by application of 1D ^{1}H NMR, but the narrow spectral width of the ^{1}H nucleus −12 ppm, compared to 200 ppm for the ^{13}C nucleus – makes this approach not well suited for the analysis of ^{13}C-enrichments in complex mixtures. To obtain both spectral resolution and sensitivity, an alternative is the application of 2D ^{1}H–^{1}H NMR experiments where the ^{1}H signals are dispersed along two dimensions (Fig. 4). This is illustrated in Fig. 5, where the 1D and 2D NMR spectra recorded on a labelled biomass hydrolysate are displayed. The hydrolysate contained mainly the amino acids released by hydrolysis of proteins – which represented 50% of the total biomass. The signals arising from the different protonated carbons of the various amino-acids strongly overlapped in the 1D ^{1}H NMR spectrum, and for almost all of them the satellite lines from the protons bound to ^{13}C atoms could be not even distinguished. In the 2D spectrum, the signals from most protonated positions of amino-acids were well separated, and the satellites lines from the protons bound to ^{13}C nuclei were also clearly resolved.

2.2. 2D-COSY experiments

The second dimension of a 2D NMR experiment is created by introducing a mixing period in the pulse sequence. During the mixing period, the magnetization of a nucleus is transferred to another nucleus. In 2D-COSY experiments, the transfer is achieved by scalar coupling, and the signal actually detected comes from anti-phase coherences:

$$\text{COSY}: \quad I_{xa}(t1) \rightarrow \text{mixing period} \rightarrow I_{yb}S_{za} \rightarrow \text{acquisition}$$

(only the coherences giving detectable correlations are shown).

The term *anti-phase* means that the two lines of the doublet arising from the coupling between the two nuclei have opposite signs and lineshapes. After Fourier transformation, such anti-phase coherences give a signal consisting in two peaks, one negative and one positive (Fig. 4). The two opposite contributions have the same intensity, so that the total intensity of the signal is zero. They are separated by the value of the homonuclear coupling constant (J_{HH}), and magnitude correction can be applied to integrate the signal. The same behaviour holds for all components – i.e. the satellite and center lines – of the cross-peak. Because the J_{HH} has values much lower than the $^1J_{CH}$ (120–180 Hz), the splitting of the lines due to homonuclear coupling does not interfere with heteronuclear couplings, so that the satellite lines remain well separated from the center peaks. The ^{13}C-enrichment of the protonated carbon

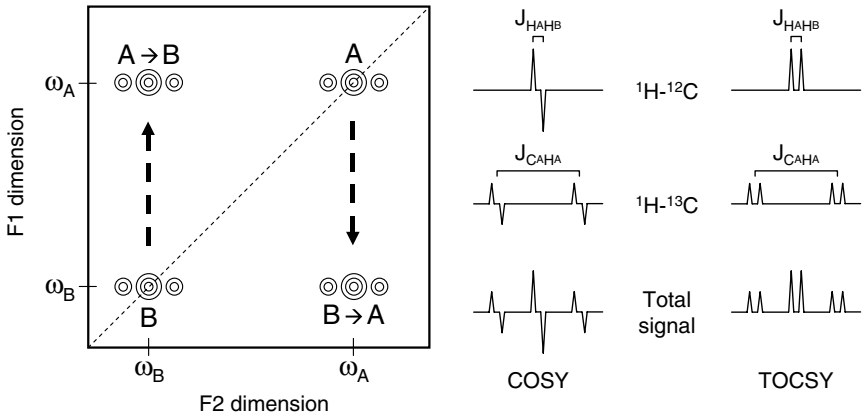

Fig. 4. Application of 2D-COSY and 2D-TOCSY to the measurement of ^{13}C-enrichments. The ^{13}C enrichment of protonated carbon can be extracted from the corresponding cross-peak(s) in 2D ^{1}H–^{1}H experiments. The cross-peak contains ^{1}H–^{13}C heteronuclear structures where the center and satellite lines correspond to ^{1}H nuclei bound to ^{12}C and ^{13}C nuclei, respectively. The satellite lines are separated one from each other by the value of the heteronuclear coupling constant (J_{CH}, ~150 Hz). The content in ^{13}C in the protonated carbon position is calculated by comparing the intensity of the satellite to the total intensity of the cross-peak. In 2D ^{1}H–^{1}H COSY experiments, each line in the cross-peak appears as an anti-phase signal where the positive and negative branches are separated by the value of homonuclear couplings (J_{HH}, ~1–7 Hz). Magnitude correction is usually applied to integrate the different signals. In 2D ^{1}H–^{1}H TOCSY experiments, in-phase signals are recorded and no magnitude correction is applied.

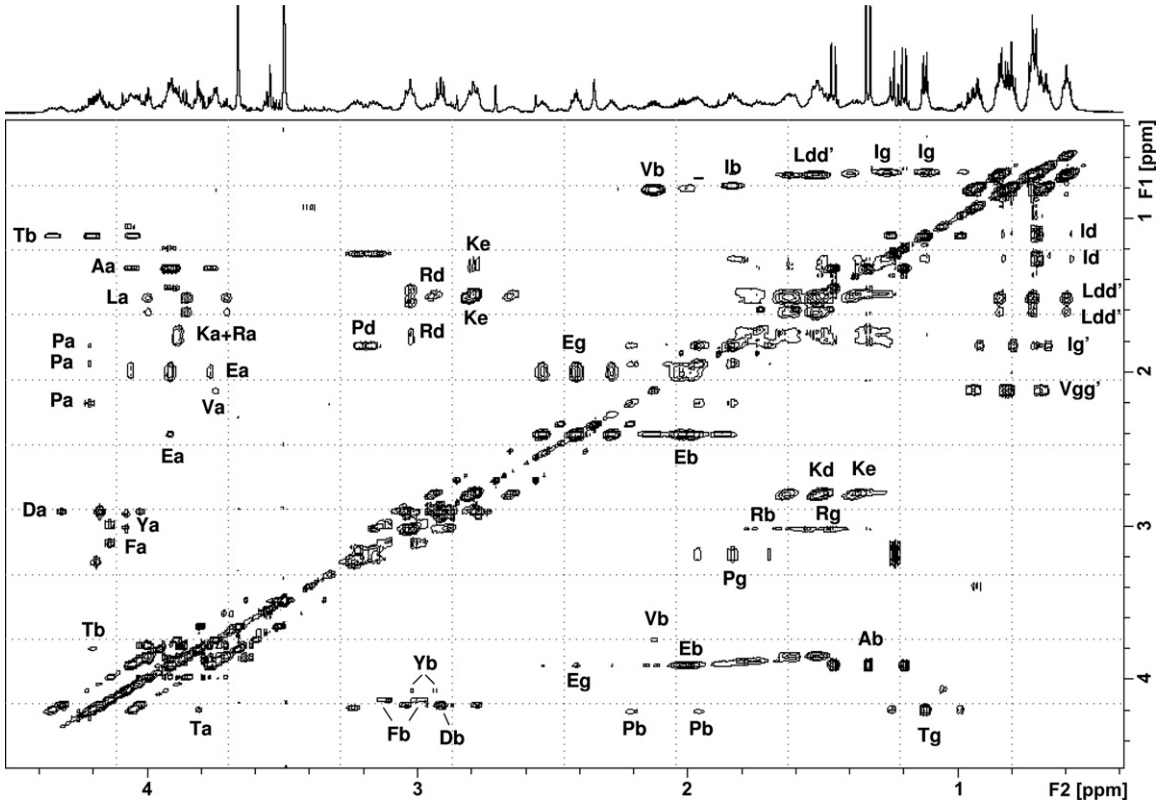

Fig. 5. 2D ZQF-TOCSY spectrum of a biomass hydrolysate from *E. coli* cells grown on 20% [U-^{13}C]-glucose +80% [1-^{13}C]-glucose. This spectrum shows an expansion of the aliphatic region of the 2D ZQF-TOCSY spectrum of the labelled sample. The sample contained mainly the amino-acids released from the hydrolysis of cellular proteins. The cross-peaks were annotated according to the corresponding protonated carbon in the amino-acids, and were annotated using the international one code letter for amino-acids, and using standard letters for the position of the protonated carbon in the molecular backbone, i.e. a, b, g, d and e for α, β, γ, δ and ε, respectively. The 1D ^{1}H NMR spectrum recorded on the sample is displayed on the top of the figure.

position can be measured by comparing the intensity of the satellite lines to the total intensity of the cross-peak in the magnitude-corrected spectrum.

Two-dimensional DQF–COSY was applied to the analysis of a mixture containing 50% [U-^{13}C]-alanine + 50% unlabelled alanine. This amino-acid is frequently consid-

ered in CLEs (it is found in biomass hydrolysates, cell extracts, culture media, etc.) and it contains chemical structures commonly encountered in metabolites. The cross-peaks observed for the $^{1}H\alpha$ of Ala in both uncorrected and magnitude-corrected spectra are shown in Fig. 3. As expected, the cross-peaks from uncorrected spectra contained anti-phase signals that were clearly detected for both the satellite and center lines (Fig. 3b), and the integral of the signal was zero. The application of magnitude correction resulted in cross-peaks with only positive signals (Fig. 3c), and the ^{13}C-enrichment could be measured from the intensity of the satellite lines relative to the total intensity of the cross-peak. The ^{13}C-enrichment of Ala Cα measured from the $^{1}H\alpha$ cross-peak displayed in Fig. 3c was only 41.5%. This was significantly lower than the value (50.6%) measured from the ^{1}H 1D NMR analysis of the same sample (Fig. 3a).

Such discrepancy between the ^{13}C-enrichments measured by 2D-DQF-COSY and ^{1}H 1D NMR experiments could be explained by two main factors: (i) the intrinsic drawbacks of magnitude correction regarding signal quantification and (ii) the effects of long-range heteronuclear couplings.

2.3. Effects of magnitude correction

Magnitude correction is a process where the module of the NMR signal is calculated from both the real and imaginary parts of the spectrum. Generally, the real part of a NMR spectrum has narrow lines but the imaginary part is broad. The module of the NMR signal is therefore much broader than the real part of the spectrum, a feature amplified by the magnitude correction process itself. In addition, the integration value is highly dependent upon the choice of the integration limits when magnitude correction is applied. Assuming the NMR signals are pure Lorentzian functions, the integral from $-\Omega$ to Ω of the real part of a NMR spectrum is $2 \times A \times \mathrm{atan}(\Omega \times \mathrm{T2})$, where A is the amplitude factor and T2 the transverse relaxation time. A finite value ($A \times \pi$) is obtained when the integration limits ($+/-\Omega$) are increased. Therefore, in a spectrum where no magnitude correction is applied, the integration limits can be objectively determined by extending the integration window until the integral does no longer increase. In magnitude corrected spectra, the integral is $2 \times A \times \ln(\Omega \times \mathrm{T2} + \sqrt{((\Omega \times \mathrm{T2})^2+1)})$. The logarithmic function increases over the entire spectrum, and no limit is reached when the integration window is enlarged. This means that the integration limits cannot be fixed objectively in magnitude-corrected spectra, which can be a potential source of quantification errors.

The effects of magnitude correction were clearly observed in the resonances of Ala $^{1}H\alpha$ displayed in Fig. 3. All lines in the $^{1}H\alpha$ resonance observed in the magnitude-corrected 2D-COSY cross-peak (Fig. 3c) were significantly broader than in the 1D ^{1}H peak (Fig. 3a) or in the uncorrected 2D-COSY cross-peak (Fig. 3b). Compared to the 1D spectrum, the spectral resolution at half- and 1%-peak height was degraded by factors $\sqrt{3}$ and 10, respectively. Line broadening resulted also in significant overlap between the satellite and center lines, since the lower intensity between the two lines in the 2D spectrum was 1000 higher than in the 1D spectrum (see from Fig. 3a and c). Such overlap was likely to lead to quantification errors, and made difficult the choice of the actual integration limits.

2.4. Effects of long-range heteronuclear couplings

The above results indicated that magnitude correction has deleterious effects on signal quantification in 2D-COSY spectra. However, these effects are not likely to fully explain the discrepancy between the ^{13}C-enrichments measured by 1D ^{1}H and 2D-COSY NMR. The difference could be explained also by effects related to long-range heteronuclear couplings ($^{LR}J_{CH}$), i. e. the couplings between a ^{1}H nucleus and a ^{13}C nucleus separated by two ($^{2}J_{CH}$) or more ($^{3}J_{CH}$, $^{4}J_{CH}$, etc.) chemical bonds. Long-range J_{CH} constants have values – a few Hz – similar to that of J_{HH} couplings between two adjacent ^{1}H nuclei. They may potentially interfere in 2D ^{1}H–^{1}H experiments in such a way that some specific ^{1}H signals are canceled, thereby minimizing the contribution of some isotopomers. To investigate the theoretical effects of $^{LR}J_{CH}$ couplings during a DQF-COSY experiment, we have simulated the behaviour of a mixture (50/50) of two spin systems mimicking unlabelled ($^{1}H_a$–$^{12}C_a$–$^{12}C_b$–$^{1}H_b$) and uniformly labelled ($^{1}H_a$–$^{13}C_a$–$^{13}C_b$–$^{1}H_b$) blocks of protonated carbons. The H_a–H_b coupling constant ($J_{H_aH_b}$) was kept constant at 5 Hz and the C_b–H_a heteronuclear constant ($^{2}J_{C_bH_a}$) was varied from 0 to 7 Hz. The transverse relaxation time was set at 0.5 s. The results are shown in Fig. 6. Both the lineshape and intensity of the satellite signals were significantly altered with the value of $^{2}J_{CH}$; meanwhile the center lines did not evolve. When $^{2}J_{C_bH_a}$ was set at the value of $J_{H_aH_b}$ – i.e. 5 Hz – the intensity of the satellite peaks was 50% lower than observed when $^{2}J_{C_bH_a}$ was set at zero. Consequently, the ^{13}C enrichment measured for the former situation was lower than expected ($0.25/0.75 = 0.33$ instead of 0.50). The difference was significant and could be explained by the evolution of the spin systems during the acquisition period. During acquisition, the active ^{1}H–^{1}H couplings – giving rise to the detected correlation – evolve as $\sin(\pi J_{H_aH_b} \times t2)$. This term is multiplied by the product of all passive couplings, $\Pi \cdot \cos(\pi J_{H_a-X} \times t2)$. The actual signal collected from the $^{1}H_a$–$^{13}C_a$–$^{13}C_b$–$^{1}H_b$ spin system, where $^{2}J_{CH} = J_{HH}$, is $0.5 \times \sin(2\pi J_{H_aH_b} \times t2)$; meanwhile the $^{1}H_a$–$^{12}C_a$–$^{12}C_b$–$^{1}H_b$ spin system is not affected.

The simulation results clearly indicated that $^{LR}J_{CH}$ couplings have significant effects on the measurement of ^{13}C-enrichments in 2D-COSY. They lead to significant errors in the measurements, especially when the values of $^{LR}J_{CH}$ get close to the values of J_{HH} (Fig. 7a). Additional simulations were performed to evaluate the measurement error

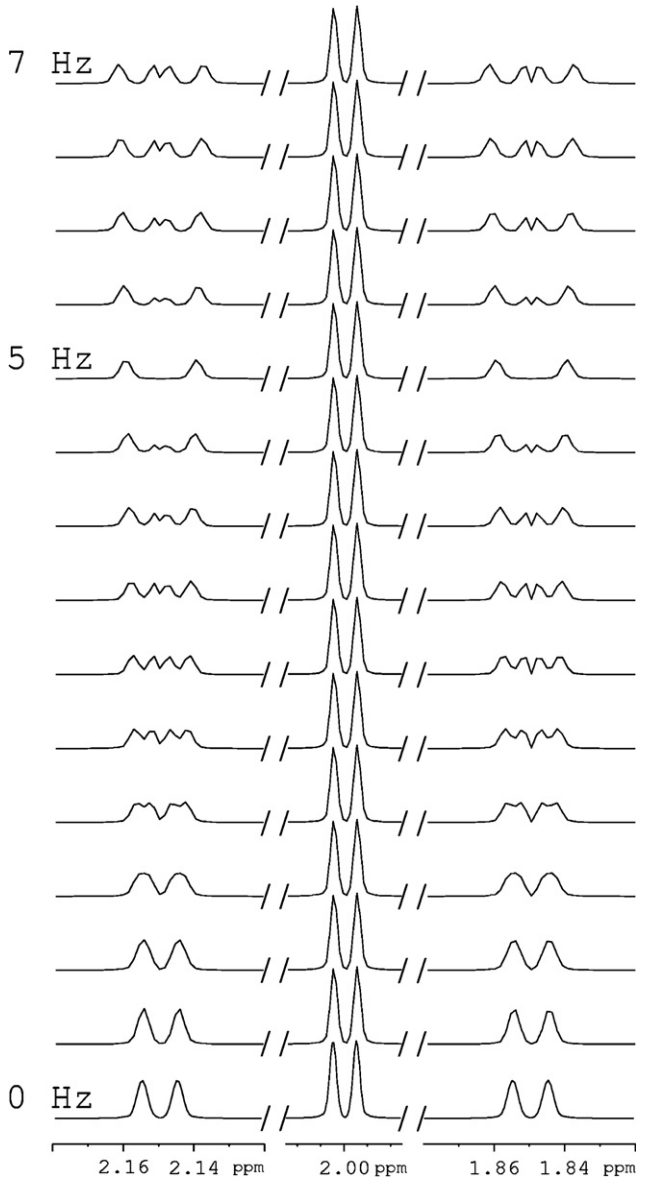

Fig. 6. Effect of long-range heteronuclear couplings on the shape of cross-peaks in 2D COSY spectra. The effects of long-range heteronuclear coupling on the shape of cross-peaks in 2D-DQF-COSY spectra were simulated for a mixture (50/50) of two spin systems corresponding to unlabelled (^1H_a–$^{12}C_a$–$^{12}C_b$–^1H_b) and uniformly-labelled (^1H_a–$^{13}C_a$–$^{13}C_b$–^1H_b) 2-carbon blocks. The $J_{H_aH_b}$ homonuclear constant between ^{1}Ha and ^{1}Hb was fixed at 5 Hz in all simulations, and the $^2J_{C_bH_a}$ heteronuclear coupling constant between ^{1}Ha and ^{13}Cb was varied from 0 to 7 Hz.

for various levels of ^{13}C-enrichment, assuming $J_{C_bH_a} = J_{H_aH_b}$. An error was observed for all enrichment values, except at 100% enrichment (Fig. 7b). The higher errors were observed for the lower enrichment values – e.g. at 10% enrichment the relative error was 47% – but at 90% enrichment, the error was still over 10%.

The simulations were run for a quite simple situation where only two spin systems were considered, but the $^{LR}J_{CH}$ coupling effects can be generalized to all spin systems for which the sum of all heteronuclear couplings acting on a ^{1}H–^{1}H correlation is greater than the J_{HH} constant. This means that the shape and intensity of each component – i.e. satellite or center lines – of a 2D-COSY cross-peak collected form a protonated carbon position can be strongly influenced by the distribution of ^{13}C atoms in the neighboring carbon positions. Three main situations can be encountered regarding the effects of $^{LR}J_{CH}$ couplings:

- A ^{1}H nucleus bound to a ^{12}C or a ^{13}C nucleus and having no magnetically interacting ^{13}C atom in the neighborhood will be not influenced.
- A ^{1}H nucleus bound to ^{13}C nucleus and having magnetically interacting ^{13}C atoms in the neighborhood will have lowered satellite lines, but the center lines would not be affected; the ^{13}C-enrichment will be underestimated.
- A ^{1}H nucleus bound to ^{12}C nucleus and having magnetically interacting ^{13}C atoms in the neighborhood will have lowered center lines, but the satellite lines would not be affected; the ^{13}C-enrichment will be overestimated.

In a true sample, all the situations are likely to occur. The different errors do not compensate one for each other, so that the cumulated error can be significant, leading to serious misinterpretation of the labelling data.

2.5. 2D-TOCSY experiments

In a 2D-TOCSY experiment (Bax and Davis, 1985), the detected signal comes from in-phase coherences (the term in-phase means that the two lines of the doublet have the same signs and lineshapes):

$$\text{TOCSY}: \quad I_{xa}(t1) \rightarrow \text{mixing period} \rightarrow I_{xb} \rightarrow \text{acquisition}$$

(only the main coherence giving detectable correlations is shown)

Because the I_{xb} coherence is responsible for signal detection in 1D ^{1}H spectra, the TOCSY signal is expected to be very close to the 1D signal. Therefore, a number of the problems encountered in COSY experiments do not apply to TOCSY experiments:

(i) The in-phase coherences give only positive signals in the TOCSY cross-peaks, and magnitude correction has not to be applied.
(ii) The heteronuclear scalar couplings are averaged to zero during the isotropic mixing period where a succession of 180° pulses is applied on the ^{1}H channel. Therefore, the effects related to long-range heteronuclear couplings can be avoided.

Therefore, most of the problems encountered in COSY are not relevant to TOCSY, and it can be expected that the latter experiment provides a more reliable method for measuring ^{13}C-enrichments. But due to the strong scalar

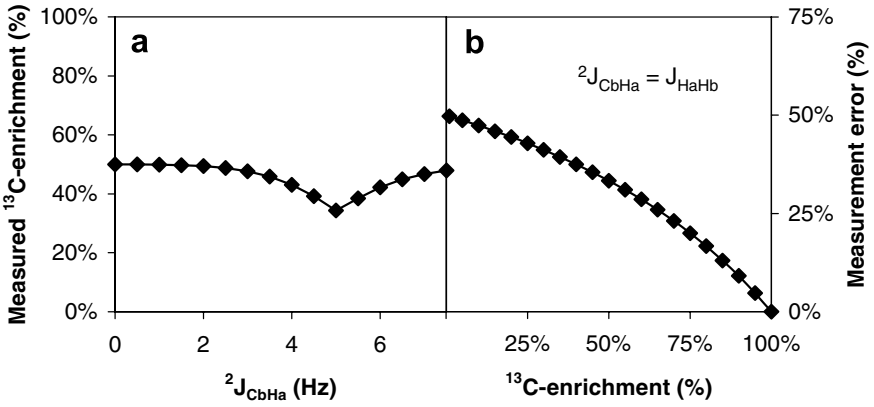

Fig. 7. Effects long-range heteronuclear couplings on the measurement of ^{13}C-enrichments from 2D DQF–COSY cross-peaks. (a) Evolution of the measured ^{13}C-enrichment with the value of the $^2J_{C_bH_a}$ heteronuclear coupling constant. The ^{13}C-enrichments were calculated from the simulated data displayed in Fig. 4, by measuring the intensity of the satellites lines relative to the total intensity of the simulated cross-peaks. (b) Evolution of the measurement error with the ^{13}C-enrichment. 2D DQF-COSY cross-peaks from mixtures of unlabelled (^1H_a–$^{12}C_a$–$^{12}C_b$–^1H_b) and uniformly-labelled (^1H_a–$^{13}C_a$–$^{13}C_b$–^1H_b) 2-carbon blocks were simulated for different mixture ratios. The $^2J_{C_bH_a}$ heteronuclear coupling constant was set equal to the value – 5 Hz – of the $^2J_{H_aH_b}$ in all simulations. The ^{13}C-enrichments were measured from the simulated cross-peaks. For each mixture ratio, the measurement error was calculated from the difference between the measured value and the theoretical value, and was expressed relative to the theoretical value.

coupling conditions applied during the mixing period, some zero-quantum coherences are also generated (Luy et al., 1999) and result in anti-phase signals in the 2D spectrum. The actual signal is a sum of in-phase and anti-phase contributions. As stated previously, the positive and negative branches of the anti-phase contributions have the same intensity, so that the total intensity of the anti-phase contributions is zero. Theoretically, the anti-phase contributions should have no effects on the integration of the cross-peak signals, and, thereby, no effects on the measurement of ^{13}C-enrichments. In practice, for small molecules such as metabolites the number of zero-quantum coherences generated for each spin system – i.e. each protonated carbon here – is such that the actual signal is severely distorted, preventing the accurate integration of the cross-peaks. Zero-quantum (ZQ) filtration can be added to the pulse sequence to remove most of the anti-phase contributions. The recent generation of ZQ filters (ZQF) based on adiabatic pulses has proved to be very efficient, and provides essentially absorptive signals (Thrippleton and Keeler, 2003).

To investigate the reliability of TOCSY to provide accurate measurements of ^{13}C-enrichments, 2D ZQF-TOCSY was applied to the analysis of the mixture of 50% [U-^{13}C]-alanine + 50% unlabelled alanine. The cross-peaks observed for the ^{1}Hα protons are shown in Fig. 3d. Because no magnitude correction was applied, the spectral resolution was equivalent to that observed in the 1D ^{1}H spectrum (Fig. 3a). A close examination of the Hα cross-peaks showed that the signal lineshapes were not fully similar to that of the 1D ^{1}H peak. The central quadruplet has the expected 1,3,3,1 height distribution in the 1D spectrum (Fig. 3a), but not in the 2D-TOCSY spectrum (Fig. 3d). This was due to small residual ZQ coherences inherent to the finite duration of the adiabatic pulses in the ZQ filters (Thrippleton and Keeler, 2003). Anyway, because the integral of signals from ZQ coherences are zero and the contribution of the latter coherences is drastically reduced by application of the ZQ filters, they did not alter the measurement of ^{13}C-enrichments. Indeed, the enrichment of Cα measured from the ^{1}Hα TOCSY cross-peak (50.4%) was in close agreement with that obtained from ^{1}H 1D NMR (50.6%).

Eventually, 2D ZQF-TOCSY was applied to the analysis of a labelled biomass hydrolysate prepared from *E. coli* cells grown on a medium containing a mixture of 80% of [1-^{13}C]-glucose and 20% of [U-^{13}C]-glucose (Fig. 5). The hydrolysate contained 16 proteinogenic aminoacids (namely, Ala, Arg, Asp, Glu, Gly, His, Ileu, Leu, Lys, Met, Phe, Pro, Ser, Thr, Tyr, Val), representing a total of 49 aliphatic and 7 aromatic protons that could be potentially detected in the 2D-^{1}H,^{1}H spectrum. Due to strong scalar coupling (e.g. Phe aromatic protons), peak overlapping (e.g. Lys and Arg), low abundance of some amino-acids (e.g. Met or His), some signals were not detected or were not exploitable for quantification purpose. However, 35 protonated carbons yielded clear cross-peaks with signal-to-noise ratios accurate for the determination of specific enrichments. The measured enrichments varied from 18.8% to 58.0%, which was fully consistent with the label input.

3. Conclusions

The reliability of 2D ZQF-TOCSY experiments to provide accurate quantitative signals from ^{13}C-labelled molecules makes it a promising technique for the purpose of measuring ^{13}C-enrichments in complex biological mixtures. Such capability offers three main advantages in the framework of CLEs. The measurement of enrichments in proton-

ated carbon positions of metabolites can be performed without need for separation of the compounds, saving time and effort. It can be applied to cell extracts, and it is likely that quite a lot of metabolic information can be derived from the 2D spectra. It allows the – positional – isotopomer approach to be conveniently extended to any combination of specifically- and uniformly-labelled substrates. The analysis of isotopomer by NMR is usually limited to uniformly-labelled substrates because the statistical analysis of ^{13}C–^{13}C in HSQC spectra needs all specific enrichments to be known. By combining 2D-TOCSY to 2D-HSQC, both specific enrichments and isotopomers can hopefully be determined (Fig. 2). Last, the approach is suitable for examining non-steady-state conditions, and therefore it can potentially be applied to investigate the dynamics of metabolic systems from time-course ^{13}C-labelling experiments.

The methodological considerations developed in this study are independent of the biological system and can apply to microbes, animals, or plants. The applicability of 2D NMR methods to the investigation of plant metabolism has been widely demonstrated, especially in the fields of metabolite profiling (Fan et al., 1997, 2001) and isotopic (^{13}C, ^{15}N) tracing of metabolism (Mesnard et al., 2002; Mesnard and Ratcliffe, 2005; Ratcliffe et al., 2001; Ratcliffe and Shachar-Hill, 2005; Shachar-Hill et al., 1996). Quantitative 2D-^{13}C,^{1}H NMR methods have been also applied for the purpose of metabolic flux analysis (Sriram et al., 2004), showing that the 2D NMR strategies that are applied for metabolic flux analysis in microbes can apply to plant systems as well (Ratcliffe and Shachar-Hill, 2006). Therefore, it is likely that 2D-^{1}H,^{1}H NMR methods such as 2D ZQF-TOCSY can be implemented for the investigation of plant systems, with the benefits mentioned above. Especially, combinations of 2D-^{13}C,^{1}H NMR and 2D-^{1}H,^{1}H NMR appear very promising tools for the detailed examination of metabolic dynamics in plants.

4. Experimental

4.1. L-alanine sample preparation

A 50% labelled alanine solution was prepared by mixing 7.5 mg unlabelled – i.e. ^{13}C at natural abundance – to 7.5 mg 99.9% [U-^{13}C]-L-alanine (Eurisotop, France). Labile protons were exchanged with deuterium by lyophilizing twice in 3 ml D_2O 99.9% (Eurisotop) and the final sample was suspended in 600 μl of 100 mM DCl (Eurisotop). The ^{13}C-enrichment measured from 1D ^{1}H NMR spectra recorded on the labelled sample was 50.6% (Fig. 3a).

4.2. Biomass sample preparation

Escherichia coli MG1655 was grown on a minimal medium containing 80% of [1-^{13}C]-glucose and 20% of [U-^{13}C]-glucose at a total concentration of 2 g l^{-1}. Batch cultures were performed at 37 °C in a 2 l stirred tank with a total partial pressure of oxygen maintained over 20% and pH was kept constant at 6.9 by addition of NaOH. Steady state cells ($OD_{600\ nm} = 1$) were harvested by centrifugation and hydrolyzed in 6 M HCl at 105 °C for 24 h. NMR measurements were carried out on hydrolysates after lyophilization and resuspension in 600 μl of 100 mM DCl.

4.3. NMR spectroscopy

1D and 2D NMR spectra were obtained on an Avance 500 MHz spectrometer (Bruker) equipped with a 5 mm z-gradient BBI probe. The data were acquired and processed using TOPSPIN® 1.3 software. The temperature was 298 K.

1D ^{1}H spectra were acquired by using a 30° pulse, a 5000 Hz sweep width and 1.6 s acquisition time. A total of 64 scans were recorded and the relaxation delay between scans was 30 s to have full signal recovery.

The ZQF-TOCSY pulse sequence was derived from a 2D TOCSY pulse sequence by adding zero quantum filters (Thrippleton and Keeler, 2003) before and after the isotropic mixing period. The ^{13}C–^{1}H heteronuclear scalar couplings were removed in the indirect dimension by a ^{13}C π refocusing pulse. DIPSI-2 TOCSY mixing sequence was applied during 25 and 50 ms (8.3 kHz), for the biomass and alanine sample, respectively. Adiabatic 180° CHIRP pulses with 10% smoothing and 20 kHz were applied during 50 ms (first pulse) and 30 ms (second pulse). A squared 0.2 G/mm gradient pulse was applied during the total length of the adiabatic pulse. At the end of the mixing period, in-plane magnetizations were defocused by a 2.6 G/mm squared purge gradient pulse. 2D spectra were obtained with quadrature phase detection in both dimensions, using TPPI method in the indirect dimension. For each 512 increments in the F1 dimension, eight transients were accumulated with the same sweep width and acquisition time as in 1D experiments. A π/2 shifted square sine-bell function was applied in the indirect dimension before Fourier transformation. To perform 2D quantification, pseudo 1D-spectra were created by summing all the rows containing the cross-peaks of interest, and were integrated like normal 1D spectra.

A standard 2D DQF-COSY extracted from the Bruker pulse program library was modified by introducing a ^{13}C 180° pulse added in the middle of the mixing period. The 2D DQF-COSY experiments were carried out using the same acquisition and processing parameters as ZQF-TOCSY experiments.

4.4. Simulation of NMR spectra

The effects of long-range heteronuclear couplings ($^{LR}J_{CH}$) on homonuclear couplings (J_{HH}) during a DQF-COSY experiment were simulated for a mixture (50/50) of two spin systems mimicking unlabelled ($^{1}H_a$–$^{12}C_a$–$^{12}C_b$–$^{1}H_b$) and uniformly labelled ($^{1}H_a$–$^{13}C_a$–$^{13}C_b$–$^{1}H_b$)

blocks of protonated carbons. The one bound heteronuclear ($J_{C_aH_a}$) and the homonuclear ($J_{H_aH_b}$) coupling constants were fixed at 150 Hz and 5 Hz, respectively. The two-bond heteronuclear coupling constant between H_a and C_b ($^2J_{C_bH_a}$) was varied from 0 to 7 Hz in 0.5 Hz steps. All the nuclei had a 0.5 s transverse relaxation time and the chemical shift difference between H_a and H_b was 2 ppm. Perfect 90° and 180° pulses were applied and the simulations were carried out assuming a 500.13 MHz magnetic field.

Additional simulations were performed to evaluate the measurement error for various levels of ^{13}C-enrichment. 2D DQF-COSY cross-peaks were simulated as above for different mixtures of unlabelled (^1H_a–$^{12}C_a$–$^{12}C_b$–^1H_b) and uniformly-labelled (^1H_a–$^{13}C_a$–$^{13}C_b$–^1H_b) 2-carbon blocks. The mixture ratios were varied from 1.1% to 100% ^{13}C-enrichment in steps of 5%. The other simulation conditions were as mentioned above except that the $^2J_{C_bH_a}$ heteronuclear coupling constant was set equal to the value – 5 Hz – of the $J_{H_aH_b}$ in all simulations. The ^{13}C-enrichments were measured from the intensity of the satellites lines relative to the total cross-peak intensity, and measurement errors were calculated from the difference between measured and theoretical values.

All the NMR simulations were performed with the NMRSIM® 4.3 software and the data were processed with TOPSPIN® 1.3 (all softwares from Bruker, Germany).

Acknowledgements

This work was supported by a Grant No. JC8099 from the French Ministry for Education & Research. The work was carried out at MetaSys, the Metabolomics & Fluxomics Center at the Laboratory of Biotechnology and Bioprocess Engineering (Toulouse, France), which is supported by the Région Midi-Pyrénées and the European Regional Development Fund (ERDF). The critical reading of the manuscript by A.P. Alonso was gratefully acknowledged.

References

Alonso, A.P., Vigeolas, H., Raymond, P., Rolin, D., Dieuaide-Noubhani, M., 2005. A new substrate cycle in plants. Evidence for a high glucose-phosphate-to-glucose turnover from in vivo steady-state and pulse-labeling experiments with [13C]glucose and [14C]glucose. Plant Physiol. 138, 2220–2232.

Bax, A., Davis, D.G., 1985. MLEV-17-based two-dimensional homonuclear magnetization transfer spectroscopy. J. Magn. Res. 65, 355–360.

Burgess, S.C., Carvalho, R.A., Merritt, M.E., Jones, J.G., Malloy, C.R., Sherry, A.D., 2001. 13C isotopomer analysis of glutamate by J-resolved heteronuclear single quantum coherence spectroscopy. Anal Biochem. 289, 187–195.

Carvalho, R.A., Jeffrey, F.M., Sherry, A.D., Malloy, C.R., 1998. C isotopomer analysis of glutamate by heteronuclear multiple quantum coherence-total correlation spectroscopy (HMQC-TOCSY). FEBS Lett. 440, 382–386.

de Graaf, A.A., 2000. Use of ^{13}C labelling and NMR spectroscopy in metabolic flux analysis. In: Barbotin, J.N., Portais, J.C. (Eds.), NMR in Microbiology Theory and Applications. Horizon Scientific Press, Wymondham, pp. 73–103.

de Graaf, A.A., Mahle, M., Mollney, M., Wiechert, W., Stahmann, P., Sahm, H., 2000. Determination of full ^{13}C isotopomer distributions for metabolic flux analysis using heteronuclear spin echo difference NMR spectroscopy. J. Biotechnol. 77, 25–35.

Eisenreich, W., Slaghuis, J., Laupitz, R., Bussemer, J., Stritzker, J., Schwarz, C., Schwarz, R., Dandekar, T., Goebel, W., Bacher, A., 2006. ^{13}C isotopologue perturbation studies of Listeria monocytogenes carbon metabolism and its modulation by the virulence regulator PrfA. Proc. Natl. Acad. Sci. USA 103, 2040–2045.

Fan, T.W., Lane, A.N., Pedler, J., Crowley, D., Higashi, R.M., 1997. Comprehensive analysis of organic ligands in whole root exudates using nuclear magnetic resonance and gas chromatography–mass spectrometry. Anal. Biochem. 251, 57–68.

Fan, T.W., Lane, A.N., Shenker, M., Bartley, J.P., Crowley, D., Higashi, R.M., 2001. Comprehensive chemical profiling of gramineous plant root exudates using high-resolution NMR and MS. Phytochemistry 57, 209–221.

Kelleher, J.K., 2001. Flux estimation using isotopic tracers: common ground for metabolic physiology and metabolic engineering. Metab. Eng. 3, 100–110.

Luy, B., Schedletzky, O., Glaser, S.J., 1999. Analytical polarization transfer functions for four coupled spins 1/2 under isotropic mixing conditions. J. Magn. Reson. 138, 19–27.

Mesnard, F., Ratcliffe, R.G., 2005. NMR analysis of plant nitrogen metabolism. Photosynth Res. 83, 163–180.

Mesnard, F., Azaroual, N., Marty, D., Fliniaux, MA., Robins, R.J., Vermeersch, G., Monti, JP., 2002. Use of 15N reverse gradient two-dimensional nuclear magnetic resonance spectroscopy to follow metabolic activity in *Nicotiana plumbaginifolia* cell-suspension cultures. Planta 210, 446–453.

Portais, J.C., Schuster, R., Merle, M., Canioni, P., 1993. Metabolic flux determination in C6 glioma cells using carbon-13 distribution upon [1-^{13}C]glucose incubation. Eur. J. Biochem. 217, 457–468.

Ratcliffe, R.G., Shachar-Hill, Y., 2005. Revealing metabolic phenotypes in plants: inputs from NMR analysis. Biol. Rev. Camb. Philos. Soc. 80, 27–43.

Ratcliffe, R.G., Shachar-Hill, Y., 2006. Measuring multiple fluxes through plant metabolic networks. Plant J. 45, 490–511.

Ratcliffe, R.G., Roscher, A., Shachar-Hill, Y., 2001. Plant NMR Spectroscopy. Prog. NMR Spectrosc. 39, 267–300.

Rontein, D., Dieuaide-Noubhani, M., Dufourc, E.J., Raymond, P., Rolin, D., 2002. The metabolic architecture of plant cells. Stability of central metabolism and flexibility of anabolic pathways during the growth cycle of tomato cells. J. Biol. Chem. 277, 43948–43960.

Schmidt, K., Norregaard, L.C., Pedersen, B., Meissner, A., Duus, J.O., Nielsen, J.O., Villadsen, J., 1999. Quantification of intracellular metabolic fluxes from fractional enrichment and ^{13}C–^{13}C coupling constraints on the isotopomer distribution in labeled biomass components. Metab. Eng. 1, 166–179.

Shachar-Hill, Y., Pfeffer, P.E., Germann, M.W., 1996. Following plant metabolism in vivo and in extracts with heteronuclear two-dimensional nuclear magnetic resonance spectroscopy. Anal Biochem. 243, 110–118.

Shulman, R.G., Rothman, D.L., 2001. ^{13}C NMR of intermediary metabolism: implications for systemic physiology. Annu. Rev. Physiol. 63, 15–48.

Sriram, G., Fulton, D.B., Iyer, V.V., Peterson, J.M., Zhou, R., Westgate, M.E., Spalding, M.H., Shanks, J.V., 2004. Quantification of compartmented metabolic fluxes in developing soybean embryos by employing biosynthetically directed fractional (13)C labeling, two-dimensional [(13)C, (1)H] nuclear magnetic resonance, and comprehensive isotopomer balancing. Plant Physiol. 136, 3043–3057.

Szyperski, T., 1995. Biosynthetically directed fractional ^{13}C-labeling of proteinogenic amino acids. Eur. J. Biochem. 232, 433–448.

Szyperski, T., 1998. ^{13}C NMR, MS and metabolic flux balancing in biotechnology research. Q. Rev. Biophys. 31, 41–106.

Thrippleton, M.J., Keeler, J., 2003. Elimination of zero-quantum interference in two-dimensional NMR spectra. Angew. Chem., Int. Ed. 42, 3938–3941.

Wiechert, W., 2001. ^{13}C Metabolic flux analysis. Metab. Eng. 3, 195–206.

Wittmann, C., Heinzle, E., 2001. Modeling and experimental design for metabolic flux analysis of lysine-producing Corynebacteria by mass spectrometry. Metab. Eng. 3, 173–191.